Gyrokinetic simulations using a delta-f approach with an evolving background Maxwellian

M. Murugappan, L. Villard, S. Brunner, G. di Giannatale

Ecole Polytechnique Fédérale de Lausanne (EPFL), Swiss Plasma Center (SPC), CH-1015 Lausanne, Switzerland

This work focuses on simulating turbulence in the core and edge transitioning region using the gyrokinetic particle-in-cell (PIC) method. For plasma edge simulations, the distribution f deviates significantly from its initial state, violating the $|\delta f|/|f_0| \ll 1$ condition of the delta-f approach for noise reduction. An attempt to retain the advantage of the delta-f approach is made via a time-dependent background f_0, evolving at a slower time-scale than that of the fluctuations.

Time-dependent background

Let the delta-f splitting be

$$f = f_0 + \delta f(\vec{R}, v_\parallel, \mu, t), \qquad f_0(\hat{\psi}_0, \mathscr{E}, t) = \frac{\hat{n}_0(\hat{\psi}_0, t)}{[2\pi \hat{T}_0(\hat{\psi}_0, t)/m]^{3/2}} \exp\left[-\frac{\mathscr{E}}{\hat{T}_0(\hat{\psi}_0, t)}\right], \quad (1)$$

where $\mathscr{E}$ is the kinetic energy, and $\vec{R}$, $v_\parallel$ and $\mu = mv_\perp^2/2B$ are the gyrocenter position, parallel velocity, and magnetic moment, respectively. Specifically, $\mathscr{E} = mv_\parallel^2/2 + \mu B$, with B the magnitude of the local field. $\hat{\psi}_0$ is a function [1] of the canonical toroidal momentum $\psi_0 = \psi + \frac{v_\parallel}{\Omega_i} F(\psi)$, $\mathscr{E}$ and μ, with Ω_i the ion cyclotron frequency, ψ the poloidal flux, and F the poloidal current flux. As defined in Eq. 1, the background f_0 of a given species has a near Maxwellian form, and its time-dependence comes from the evolving background 'density' $\hat{n}_0$ and 'temperature' $\hat{T}_0$ profiles. These profiles are not exactly the corresponding particle flux-surface-averaged (f.s.a.) functions of the flux coordinate ψ, due to the dependence of $\hat{\psi}_0$ on the velocity variables.

As the adaptive scheme is entirely one-dimensional in ψ, let $\langle\cdot\rangle$ be the flux-surface-averaging operator, and let $\langle n_0\rangle(\psi,t)$ and $\langle E_{k0}\rangle(\psi,t)$ be the f.s.a. density and kinetic energy density respectively. The time-evolution of these functions are dictated by the ad-hoc equations [2]:

$$\frac{\partial \langle n_0\rangle}{\partial t} = \alpha_n \overline{\left\langle \int \mathrm{d}^3 v \delta f \right\rangle}, \qquad \frac{\partial \langle E_{k0}\rangle}{\partial t} = \alpha_E \overline{\left\langle \int \mathrm{d}^3 v \delta f \mathscr{E} \right\rangle},$$

where $\int \mathrm{d}^3 v$ stands for the integration over the velocity variables, the coefficients $\alpha_{n,E}$ the user-defined rates of relaxation, and $\overline{A}$ indicates time-averaging between adaptation steps of a quantity A. Finally, $\hat{n}_0$ and $\hat{T}_0$ in Eq. 1 are updated via the relations

$$\langle E_{k0}\rangle = \frac{3}{2}\langle n_0\rangle\langle T_0\rangle, \qquad \hat{n}_0(\psi,t) = \langle n_0\rangle(\psi,t), \qquad \hat{T}_0(\psi,t) = \langle T_0\rangle(\psi,t).$$

For an adaptation scheme using a local f.s.a. Maxwellian $f_0(\psi,\mathscr{E},t)$, the last two equations would be exact, while for a canonical Maxwellian as in Eq. 1, $\hat{\psi}_0 \approx \psi$. Of course, once f_0 is updated, δf must then be modified to satisfy the Vlasov equation $\mathrm{d}f/\mathrm{d}t = 0$.

Under the delta-f approach with a time-dependent f_0, the field equation for the self-consistent electrostatic potential ϕ is given by the quasi-neutrality equation assuming here a single ionic species and hybrid electrons [3]:

$$\begin{aligned} & \alpha_P \frac{e n_{e0}}{T_{e0}}(\phi - \langle\phi\rangle) - \nabla_\perp \cdot \left(\frac{m_i n_{i0}}{eB^2}\nabla_\perp \phi\right) \\ = & \int \mathrm{d}\alpha\, \mathrm{d}^3R\, \mathrm{d}v_\parallel\, \mathrm{d}\mu\, \{B^\star_\parallel[\delta f_i(\vec{R},v_\parallel,\mu,t) + \Delta f_{i0}]\delta[\vec{R}+\vec{\rho}_L-\vec{r}]\} \\ & -\delta n_{e,T} - \delta n_{e,P}|_{(m,n)=(0,0)} - \Delta n_{e0}, \end{aligned} \tag{2}$$

where α_P is the fraction of passing electrons, $\vec{\rho}_L$ the gyroradius, $\delta n_{e,T}$ the perturbed density for the drift-kinetic trapped electrons, $\delta n_{e,P}|_{(m,n)=(0,0)}$ the zonal contribution of the kinetic passing electrons [4], and $\Delta f_{i0} = f_{i0}(\hat{\psi}_0,\mathscr{E},t) - f_{i0}(\hat{\psi}_0,\mathscr{E},0)$. As the background profiles are evolved over time, so do the corresponding profiles on the left-hand-side (LHS), and the correction Δ-terms for the right-hand-side (RHS) of Eq.2 must be added for consistency.

Results

Following a previous work considering a simple sheared slab geometry [5], the global gyrokinetic PIC code in toroidal geometry ORB5[3] is used to perform simulations with evolving f_0. For simplicity, simulations are further restricted to be electrostatic and collisionless and with a single ion species. The ideal MHD magnectic equilibrium is generated by the coupled CHEASE code [6] based on the TCV equilibrium shot #43516 with aspect ratio $R/a = 3.64$, elongation $\kappa = 1.44$ and triangularity $\delta = 0.20$ at the last closed flux surface. The safety factor is quadratic, $q(s) = q_0 + (q_{edge} - q_0)s^2$, with $q_0 = 0.78$ and $q_{edge} = 3.29$. Here, $s = \sqrt{\psi/\psi_{edge}}$. The reference surface for normalisation is at the edge, $s_0 = 1.0$, and $\rho_\star(s_0) = \rho_i(s_0)/a = 1/245$, where a is the minor radius and ρ_i is the thermal ion larmor radius. All initial background temperature profiles are defined by [7]

$$T_0(\rho_V) = \begin{cases} a_0 + a_2\rho_V^2 & 0 \le \rho_V < \rho_{core} \\ [T_1 + \mu_T(1-\rho_{ped})]\exp[-\kappa_T(\rho_V - \rho_{ped})] & \rho_{core} \le \rho_V < \rho_{ped} \\ T_1 + \mu_T(1-\rho_V) & \rho_{ped} \le \rho_V \le 1 \end{cases}$$

where $\rho_V = \sqrt{V(\psi)/V(\psi_{edge})}$ is a radial coordinate, a_0 and a_1 are parameters for a C^2-continuous extrapolation to the magnetic axis, and ρ_{core}, ρ_{ped}, T_1, κ_T and μ_T are user-defined parameters. The background density profiles are similarly initialised with corresponding parameters.

Two cases are briefly presented here: (1) A 'flux-driven' Ion Temperature Gradient (ITG) induced turbulence simulation, with adaptive ion temperature and adiabatic electrons, (2) A 'temperature-gradient-driven' Trapped Electron Mode (TEM) induced turbulence simulation, with the hybrid electron model and adaptive densities. These cases will henceforth be known as the ITG- and TEM- cases respectively. Initial profile parameters for the ions of the ITG-case are $\rho_{core} = 0.4431$, $\rho_{ped} = 0.8$, $T_1^i = 1$, $\kappa_T^i = 2.3$, $\mu_T^i = 12$, $n_1^i = 1$, $\kappa_n^i = 3.1$ and $\mu_n^i = 5$. The adiabatic electrons have identical corresponding parameters. The parameters of the TEM-case are $\rho_{core} = 0.4016$, $\rho_{ped} = 0.8$, $T_1^i = 1$, $\kappa_T^i = 2.3$, $\mu_T^i = 6$, $n_1^i = 1$, $\kappa_n^i = 2.3$ and $\mu_n^i = 5$ for the ions, and $T_1^e = 1$, $\kappa_T^e = 2.5$, $\mu_T^e = 10$, $n_1^e = 1$, $\kappa_n^e = 2.3$ and $\mu_n^e = 5$ for the hybrid electrons. The heat source used for the ITG-case is that with five times the input power of the corresponding temperature-gradient-driven run, peaked at $s = 0.6$. Adaptive rates α_E and α_n are set to 1% of the maximum linear growth rates of the ITG- and TEM- cases, $0.0014\Omega_i$ and $0.0042\Omega_i$, respectively.

The Signal-to-Noise Ratio (SNR) [8] diagnostic measures the ratio of the energy in the field-aligned Fourier modes over that in the non-field-aligned in the RHS of Eq. 2. This diagnostic however does not include the zonal component, which may accumulate noise, in the signal band. For the ITG-case, one sees from Fig.1a that adaptive cases maintain sufficiently high (~ 10) SNR values over long periods of simulation time. Furthermore, it shows that the same simulation can be carried out the number of markers, from $N_p = 256$M to $N_p = 128$M. Fig. 1b shows that the ion temperature profile has stopped evolving around time $\Omega_c t \approx 285000$ for the non-adapted case, due to the accumulation of noise. On the other hand, all cases where f_0 was adapted converged to the same profile. For the TEM-case, Fig.1c shows again a slower drop of SNR values for the adapted cases compared to f_0 kept fixed. As all cases exhibit good SNR values, all time-averaged ion density profiles converged for this simulated time, as shown in Fig.1d. All figures show that, for adapted cases, modifications to Eq. 2 do not change the final results significantly. We have implemented and tested and adaptive control variate scheme which, for all cases explored, shows its effectiveness in controlling sampling noise, and is thus particularly adapted to long time scale simulations involving profiles with large deviations from their initial states.

Acknowledgements

This work is part of the EUROfusion 'Theory, Simulation, Validation and Verification' (TSVV) Task, and has been carried out within the framework of the EUROfusion Consortium, partially funded by the European Union via the Euratom Research and Training Programme (Grant Agreement No 101052200 — EUROfusion). The Swiss contribution to this work has been

(a) ITG-case: SNR

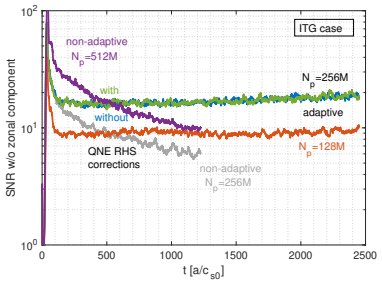

(b) ITG case: Ion temperature gradient

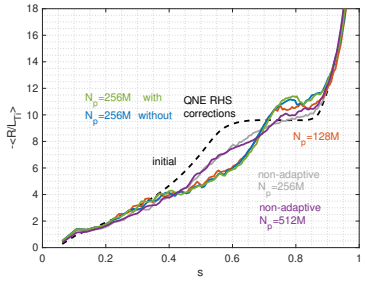

(c) TEM-case: SNR

(d) TEM case: Ion density

Figure 1: SNR diagnostics (a) and (c), and profiles (b) and (d), for the ITG- and TEM- cases, with time averaging windows $[1000, 1200]c_s t/a$ and $[200, 250]c_s t/a$ respectively. `Np` indicates marker number and `RHS` and `LHS` indicate the inclusion of the Δ-correction term on the RHS, and profile update on the LHS, of the QNE Eq.2 respectively. Dashed curves indicate initial profiles.

funded by the Swiss State Secretariat for Education, Research and Innovation (SERI). Views and opinions expressed are however those of the author(s) only and do not necessarily reflect those of the European Union, the European Commission, or SERI. Neither the European Union nor the European Commission can be held responsible for them. This work is also supported by a grant from the Swiss National Supercomputing Centre (CSCS) under project IDs s1067 and ch14, and was partly supported by the Swiss National Science Foundation.

References

[1] P. Angelino et al, Phys. Plasmas **13**, 052304 (2006)

[2] S. Brunner, E. Valeo, and J.A. Krommes, Phys. Plasmas **6**, 4504 (1999)

[3] E. Lanti et al, Comput. Phys. Commun. **251**, 107072 (2020)

[4] Y. Idomura, J. Comput. Phys. **313**, 511-531 (2016)

[5] M. Murugappan et al, Phys. Plasmas **29**, 103904 (2022)

[6] H. Lütjens, A. Bondeson and O. Sauter, Comput. Phys. Commun. **97** 219 (1996)

[7] O. Sauter et al, Phys. Plasmas **21**, 055906 (2014)

[8] B.F. McMillan et al, Comput. Phys. Commun. **181** 715 (2010)